Published online 9 May 2011 *Nucleic Acids Research, 2011, Vol. 39, No. 15* **6511–6522**
doi:10.1093/nar/gkr297

Analyses of the yeast Rad51 recombinase A265V mutant reveal different *in vivo* roles of Swi2-like factors

Peter Chi[1], YoungHo Kwon[1], Mari-Liis Visnapuu[2], Isabel Lam[3], Sergio R. Santa Maria[3], Xiuzhong Zheng[3], Anastasiya Epshtein[3], Eric C. Greene[2,4], Patrick Sung[1] and Hannah L. Klein[3,*]

[1]Molecular Biophysics and Biochemistry, Yale University School of Medicine, 333 Cedar Street, New Haven, CT 06520, [2]Department of Biochemistry and Molecular Biophysics, Columbia University Medical Center, [3]Department of Biochemistry and NYU Cancer Institute, New York University School of Medicine, 550 First Avenue, New York, NY 10016 and [4]Howard Hughes Medical Institute, 650 West 168th Street, New York, NY 10032 USA

Received March 11, 2011; Revised April 11, 2011; Accepted April 13, 2011

ABSTRACT

The *Saccharomyces cerevisiae* Swi2-like factors Rad54 and Rdh54 play multifaceted roles in homologous recombination via their DNA translocase activity. Aside from promoting Rad51-mediated DNA strand invasion of a partner chromatid, Rad54 and Rdh54 can remove Rad51 from duplex DNA for intracellular recycling. Although the *in vitro* properties of the two proteins are similar, differences between the phenotypes of the null allele mutants suggest that they play different roles *in vivo*. Through the isolation of a novel *RAD51* allele encoding a protein with reduced affinity for DNA, we provide evidence that Rad54 and Rdh54 have different *in vivo* interactions with Rad51. The mutant Rad51 forms a complex on duplex DNA that is more susceptible to dissociation by Rdh54. This Rad51 variant distinguishes the *in vivo* functions of Rad54 and Rdh54, leading to the conclusion that two translocases remove Rad51 from different substrates *in vivo*. Additionally, we show that a third Swi2-like factor, Uls1, contributes toward Rad51 clearance from chromatin in the absence of Rad54 and Rdh54, and define a hierarchy of action of the Swi2-like translocases for chromosome damage repair.

INTRODUCTION

Rad54 and Rdh54 are members of the Swi2 protein family. These evolutionarily conserved proteins possess dsDNA-dependent ATPase activity that fuels their translocation on dsDNA, resulting in DNA supercoiling and transient strand unwinding. Both proteins physically interact with the recombinase Rad51 and synergize with the Rad51–ssDNA nucleoprotein filament to promote D-loop formation, DNA branch migration and chromatin remodeling, all of which are essential steps in homologous recombination (HR) (1). Interestingly, Rad54 and Rdh54 both can remove Rad51 from dsDNA *in vitro*. The ability to dissociate the Rad51–dsDNA complex has been postulated to be important for releasing Rad51 from bulk chromatin, to ensure that a sufficient pool of free recombinase is available for repair and to prevent the accumulation of toxic Rad51–DNA intermediates. Moreover, removal of Rad51 by Rad54 and Rdh54 may be necessary to allow access of a DNA polymerase to the primer terminus in the newly made D-loop during HR. *RAD54* and *RDH54* likely serve distinct functions in mitotic and meiotic recombination, as mutants have distinct phenotypes (2–4). *rad54Δ* mutants are sensitive to DNA damaging agents and have significant reduction in mitotic recombination whereas *rdh54Δ* are only slightly sensitive to DNA damage and have a modest reduction in interchromosomal recombination, but are not affected in intrachromosomal recombination. *rdh54Δ* diploids have

*To whom correspondence should be addressed. Tel: +1 212 263 5778; Fax: +1 212 263 8166; Email: hannah.klein@nyumc.org
Present addresses:
Peter Chi, Institute of Biochemical Sciences, National Taiwan University, No. 1, Sec. 4, Roosevelt Road, Taipei, 10617 Taiwan (R.O.C.).
Isabel Lam, Memorial Sloan-Kettering Cancer Center, 1275 York Avenue, New York, NY 10065, USA.
Mari-Liis Visnapuu, McKinsey & Co., Inc., 55 East 52nd Street, New York, NY 10022, USA.

The authors wish it to be known that, in their opinion, the first four authors should be regarded as joint First Authors.

significant meiotic recombination defects and are delayed in the repair of meiotic double strand breaks whereas *rad54Δ* diploids does not show a delay in the repair of meiotic double strand breaks, although spore viability is reduced.

Even though both Rad54 and Rdh54 can dissociate Rad51 from dsDNA *in vitro* (5,6), whether these proteins remove Rad51 from chromatin *in vivo* and the functional significance and relative contributions of Rad54 and Rdh54 toward Rad51 clearance from chromatin remain unanswered. *In vivo*, *RAD54* has a more important role than *RDH54* in the recombinational repair of methyl methanesulfonate (MMS) damaged DNA and gaps that occur from replication across a damaged DNA template, as seen by the strong MMS sensitivity of *rad54* mutants, while *rdh54* mutants show only a modest sensitivity (3,4). In a recent study we have found that Rdh54 has a critical role in removing Rad51 from chromatin when Rad51 is expressed in excess, while Rad54 has only a minor role in this regard (7). In contrast, following irradiation damage, Rad51 foci persist in *rad54* mutants, but not in *rdh54* mutants (7). Likewise, we do not yet know whether Uls1, another Swi2 family member that was originally identified based on its two-hybrid interaction with the meiotic recombinase Dmc1, also plays a role in Rad51 clearance from chromatin (8). *ULS1* has no known role in DNA repair, as deletion of the gene does not render cells sensitive to DNA damaging agents, although it appears to play a role in removing excess Rad51 from chromatin (7). Here, we show synthetic growth deficiency and DNA damage sensitivity of double and triple mutants of the aforementioned Swi2-like factors that can be efficiently suppressed by deleting *RAD51*. In congruence with this, a genomic suppressor of the *rad54Δ uls1Δ* mutant defects is shown to harbor a mutation, *A265V,* in *RAD51*. We provide evidence that the suppressor activity of *rad51A265V* stems from the combined effect of this mutation on the affinity of Rad51 for DNA and the accelerated removal of the mutant rad51 protein by Rdh54 from dsDNA.

Taken together, our results provide compelling evidence for a cytotoxic effect of gratuitous Rad51–dsDNA complexes and suggest that Rad54, Rdh54 and Uls1 all contribute toward clearance of these toxic nucleoprotein complexes in a hierarchical fashion. Additionally, our results suggest that Rad54 and Rdh54 recognize different Rad51–dsDNA complexes *in vivo*.

MATERIALS AND METHODS

Spot assays on MMS-supplemented plates

Yeast cultures were incubated overnight at 30°C in YPD medium. After determining cell density, the cultures were adjusted to 10^7 cells/ml and then serially diluted. Aliquots of 4 µl from the serial dilutions were spotted onto SC or SC-containing MMS at the indicated concentration. SC plates containing MMS were made directly before use. The plates were then incubated at 30°C for 5–6 days.

Screen for suppressors of *rad54 uls1* MMS sensitivity

The *rad54Δ uls1Δ* strain used for EMS mutagenesis is HKY1287-11B *MAT***a** *rad54::LEU2 uls1::KANMX leu2-3, 112 his3-11, 15 ade2-1 ura3-1 trp1-1 can1-100 hom3-10 RAD5*. For EMS mutagenesis, cells were grown overnight at 30°C, collected and washed twice with water and resuspended in an equal volume of 0.1 M sodium phosphate buffer (pH 7). The exact cell density was determined with a hemacytometer and adjusted to 2×10^8 cells/ml. Two 1-ml aliquots were made, and 0.5 µl EMS (Sigma) was added to one aliquot, while the other aliquot served as control. The tubes were vortexed vigorously before incubating for 1 h at 30°C with agitation. After incubation, the cells were collected and washed three times with 8 ml 5% sodium thiosulfate, and once with sterile distilled water. The cells were then resuspended in 5 ml YPD, and incubated for 3 h to allow cells to express the mutant proteins. After outgrowth, 10^6 EMS-treated and control cells were plated onto YPD plates containing 0.004% MMS. In addition, 10^4, 10^2 and 10^1 EMS-treated and control cells were plated onto YPD to estimate the percentage cell death resulting from the EMS mutagenesis protocol. Colonies growing on YPD were counted after 36 h of incubation at 30°C, and percent survival was calculated to be ~25%.

Colonies growing on 0.004% MMS after 7 days of incubation at 30°C were streaked onto fresh 0.004% MMS plates to yield single colonies and compared to growth of *rad54Δ*, *uls1Δ* and *rad54Δ uls1Δ* strains. Mutants that were less sensitive to 0.004% MMS than the *rad54Δ uls1Δ* double mutant were screened for growth in 0.0025% MMS to confirm resistance to levels of MMS at which *rad54Δ uls1Δ* is not viable. Colonies with significant growth in 0.0025% MMS were chosen as putative suppressors of *rad54Δ uls1Δ* MMS sensitivity. Suppressor-containing strains were crossed several times to a wild-type strain to recover the suppressor mutation in a *RAD54 ULS1* background and to eliminate any unlinked mutations that might have arisen during the mutagenesis.

Sequencing of *RAD51*

Primers 5′CATATCCCACGACTAGGCCA3′ and 5′CAT GGGTGACAGACAATACG3′ were used to amplify the *RAD51* gene from yeast strains containing putative suppressors of *rad54Δ uls1Δ*. The PCR product was sequenced and a mutation at base 794 changing C to T or amino acid residue 265 changing alanine to valine was found in *RAD51*.

Reconstruction of the *rad51 A265V* mutation

The rad51 A265V mutant allele was introduced into an unmutagenized wild-type strain to replace the endogenous *RAD51* allele. A 1.7-kb DNA fragment including the *rad51 A265V* open reading frame was amplified using primers SSM93 (5′ CGGGGTACCCGGGGATCCCAC GACTAGGCCACAC) and SSM94 (5′ GCCAAGCTTG CATGCCTGCAGGAGGAAGTAGTCATC) from genomic DNA of a mutant yeast strain. The PCR

product was then introduced into vector YIplac211 as BamHI–PstI fragment to yield the integration construct pHK440. pHK440 was then cut with the SpeI restriction endonuclease and used to transform yeast cells to Ura^+. Positive transformants were then grown on 5-FOA-containing medium and the resulting clones confirmed for the *rad51 A265V* mutation by DNA sequencing.

Recombination assays

Recombination assays for haploid intragenic recombination and diploid intragenic heteroallelic recombination were performed as previously described (3). Recombination rates were determined by the method of the median (9).

Protein purification

Rad51 and rad51 A265V proteins were expressed in the *rad51Δ* strain LSY411 by the use of the *PGK* promoter in plasmid pMA91 (2 μ, *PGK, leu-2 d*) (10) and were purified to near homogeneity, following our published protocol (11). His_6-tagged Rad54 or Rdh54 was expressed in *Escherichia coli* and purified to near homogeneity as described (5,12).

DNA substrates

The ϕX replicative form I DNA was purchased from Gibco/BRL. Topologically relaxed ϕX DNA was prepared by treatment with calf thymus topoisomerase I (Invitrogen), as described previously (13). For DNA mobility shift assay, the 80-mer Oligo 1–5′ TTATATCC TTTACTTTGAATTCTATGTTTAACCTTTTACTTAT TTTGTATTAGCCGGATCCTTATTTCAATTATGTT CAT-3′ was 5′-end labeled with [γ-^{32}P] ATP (Amersham Bioscience) and polynucleotide kinase (Roche) and separated from the unincorporated ATP using a Spin 6 column (Bio-Rad). To generate radiolabeled dsDNA, radiolabeled Oligo 1 was annealed to its exact complement, Oligo 2. The resulting duplex was purified from a 10% polyacrylamide gel by overnight diffusion at 4°C into TE buffer (20 mM Tris–HCl, pH 7.5, 0.5 mM EDTA).

For the D-loop assay, the 90-mer oligonucleotide D1 (14), being complementary to pBluescript SK DNA from position 1932 to 2022, was 5′-end labeled and then purified using the MERmaid Spin Kit (Bio101). The 600 base pairs biotinylated dsDNA used for monitoring Rad51 removal was prepared by PCR amplification of pBluscript SK DNA using the 5′-biotinylated primer 1 and non-biotinylated primer 2, as described previously (5). The amplified DNA was deproteinized by phenol–chloroform extraction, ethanol precipitated and dissolved in TE. The biotinylated dsDNA was immobilized on streptavidin magnetic beads (Roche Molecular Biochemicals), as described previously, to give 50 ng of the biotinylated DNA per microliter of suspended volume (5). The 83-mer 5′- TTTATATCCTTTACTTTA TTTTCTATGTTTATTCATTTACTTATTTTGTATTA TCCTTATACTTATTTACTTTATGTTCATTT-3′ ssDNA was used as the Rad51 trap.

DNA mobility shift assay

The ^{32}P-labeled 80-mer ssDNA (4.5 μM nucleotides) or dsDNA (4.5 μM base pairs) was incubated with the indicated amounts of Rad51 or rad51A265V for 5 min at 37°C in 10 μl of buffer B (35 mM Tris–HCl at pH 7.5, 1 mM DTT, 50 mM KCl, 100 μg/ml BSA) containing 2 mM ATP and the indicated concentration of $MgCl_2$. The reaction mixtures were resolved in 10% polyacrylamide gels in TA buffer (40 mM Tris–acetate, pH 7.5) at 4°C. The gels were dried onto a sheet of DEAE paper and then subject to phosphorimaging analysis.

DNA topology modification reaction

Topologically relaxed ϕX dsDNA (10 μM based pairs) was incubated with the indicated amount of Rad51 or rad51A265V in 9.6 μl buffer B containing 2 mM ATP and the indicated concentration of $MgCl_2$ for 5 min, followed by the addition of 3 units of calf thymus topoisomerase I (Invitrogen) in 0.4 μl. Reaction mixtures were incubated for 15 min at 37°C and then deproteinized with 0.5% SDS and 0.5 mg/ml proteinase K for 10 min. Samples were resolved in 0.8% agarose gels run in TAE buffer (40 mM Tris–acetate, pH 7.5, 0.5 mM EDTA) at 23°C, and the DNA species were stained with ethidium bromide (2 μg/ml in water) for 1 h. After being destained in water at 4°C for 24 h, the gels were analyzed in a gel documentation station (Bio-Rad).

D-loop assay

The ^{32}P-labeled 90-mer ssDNA (2.4 μM nucleotides) was incubated with the indicated amounts of Rad51 or rad51 A265V in 10.5 μl buffer B containing an ATP-regenerating system and 5 mM $MgCl_2$ for 5 min at 37°C. Rad54 (140 nM) or Rdh54 (300 nM) was then added in 1 μl, followed by a 1-min incubation at 30°C. The D-loop reaction was initiated by adding pBluescript replicative form I DNA (35 μM base pairs) in 1 μl. The reaction mixtures were incubated for 5 min at 30°C, deproteinized and processed for electrophoresis in 0.9% agarose gels in TAE buffer (40 mM Tris–acetate, pH 7.5 0.5 mM EDTA). The gels were dried onto a sheet of DEAE paper and the radiolabeled D-loop was visualized and quantified in the phosphorimager.

ATPase assay

Rad51 or rad51 A265V (4 μM each) was incubated with 100 μM ATP, 0.1 μCi/μl [γ-^{32}P] ATP at 37°C in a 10 μl buffer containing 40 mM Tris–HCl pH 7.5, 1 mM DTT, 100 ng/μl BSA, 50 mM KCl, 2 or 5 mM $MgCl_2$ (as indicated) in the presence of ϕX 174 viral (+) strand (30 μM nucleotides) or replicative form I DNA (30 μM base pairs) or in the absence of DNA. Aliquots (2 μl) were drawn at the indicated times and mixed with an equal volume of 500 mM EDTA to stop the reaction. After thin layer chromatography in polyethyleneimine sheets (J.T. Baker Inc.), the level of ATP hydrolysis was determined by phosphorimaging analysis of the chromatography plate (14).

Assay to monitor Rad51 removal from DNA

Rad51 or rad51 A265V (3.7 μM) was incubated with magnetic beads containing biotinylated dsDNA (15 μM base pairs) in 18 μl buffer B containing 2 mM ATP, 5 mM $MgCl_2$ and an ATP-regeneration system for 5 min at 37°C. After the incorporation of the indicated amounts of Rad54 or Rdh54 in 1 μl and a 3-min incubation at 23°C, the reaction was completed by adding 83-mer ssDNA (150 μM nucleotides), as Rad51 trap, in 1 μl. Following a 10-min incubation at 30°C, the beads were captured with the Magnetic Particle Separator (Boehringer Mannheim), and the supernatant was set aside. Bound proteins were eluted from the beads with 20 μl of 2% SDS. The various supernatant and SDS eluate (8 μl each) were analyzed by SDS–PAGE and Coomassie blue staining to determine their content of proteins.

Affinity pulldown

Rad51 or rad51 A265V (5 μg each) was incubated with His_6-tagged Rad54 or Rdh54 (5 μg each) in 30 μl buffer D (20 mM KH_2PO_4, pH 7.4, 75 mM KCl, 10% glycerol, 0.5 mM EDTA, 0.01% Igepal, 1 mM 2-mercaptoethanol) for 30 min on ice. The reaction mixture was incubated with 8 μl of Ni^{2+}-NTA agarose beads for 30 min on ice, with gentle mixing every 30 s. The beads were pelleted by centrifugation, and the supernatant was removed. After being washed twice with 30 μl buffer D containing 10 mM imidazole, the beads were treated with 20 μl of 2% SDS to elute bound proteins. The supernatant (8 μl), wash (8 μl) and SDS eluate (8 μl) were subject to SDS–PAGE and Coomassie blue staining to determine their protein contents.

Gel filtration

A Sephacryl S-400 column (30 × 1 cm) was used to analyze Rad51 and rad51 A265V with buffer C (25 mM Tris, pH 7.5, 10% glycerol, 0.5 mM EDTA, 1 mM DTT, 0.01% Igepal and 150 mM KCl) as the eluent and collecting 0.2-ml fractions. The indicated column fractions were subjected to SDS–PAGE and Coomassie blue staining. Thyroglobulin (669 kDa), and catalase (232 kDa) were used for calibrating the column.

TIRFM measurements of Rad51 nucleoprotein filament stability

Flowcells and DNA curtains were prepared essentially as described (15). The DNA substrate was a 23-kb segment of the human β-globin locus that was amplified with the Expand 20 kB^{PLUS} PCR system from human genomic DNA using forward and reverse primers that are covalently linked to biotin and digoxigenin, as described elsewhere (16). The DNA was labeled with quantum dots covalently conjugated to anti-digoxygenin Fab-fragments (Roche). Rad51 (700 μL of 1 μM, either wild-type or A265V mutant) was injected at 37°C in buffer containing 1 mM ATP and either 10 or 2 mM of $MgCl_2$, as indicated, and reactions were chased with buffer lacking Rad51. Images were recorded for 15 min at 1-s intervals. The DNA length was measured by tracking the location of the quantum dot (17). The data corresponding to filament disassembly are fit with a sigmoidal curve the slope of which is used to determine the disassembly rate, and all reported rates represent the mean obtained from three independent experiments, as described previously (16).

RESULTS

Genetic interaction of *uls1* with *rad54* and *rdh54*

The *ULS1* gene was identified in a two-hybrid screen for yeast proteins that interact with Dmc1, a meiosis-specific Rad51 homolog (8). Uls1 protein (also known as Ris1 or Tid4) is a member of the Swi2 family. Interestingly, the Uls1 protein possesses a RING finger domain suggestive of an ubiquitin ligase activity (18). The most closely related *Saccharomyces cerevisiae* proteins are Rad5 and Rad16, which are involved in post-replication repair (PRR) and nucleotide excision repair (NER), respectively.

Mutations in the homologous recombination factors Rad54 and Rdh54, which are also Swi2 family members, result in DNA damage sensitivity and reduced homologous recombination, although the *rad54* mutant is much more affected than the *rdh54* mutant. The *rad54Δ rdh54Δ* haploid double mutant grows at the same rate as the haploid *rad54*Δ strain, but diploid growth of *rad54*Δ *rdh54*Δ is greatly impaired, with clonal lethal sectors (3) (Figure 1A). Deletion of *RAD51* in the *rad54Δ rdh54Δ* diploids restored normal growth (3) (Figure 1A), suggesting that Rad51 may form toxic intermediates in these diploids. To determine if additional *SWI2* genes could be involved in avoidance of the Rad51 toxic intermediates, we focused on *ULS1*, based on its reported interaction with the Rad51-related recombinase protein Dmc1 (8). We found that a homozygous mutation of *ULS1* in the *rad54Δ rdh54Δ* diploids further aggravates growth deficiency (Figure 1A), while the haploid triple mutant strain *rad54Δ rdh54Δ uls1Δ* grows slower than single or double mutants, but without clonal lethality (7). As expected, the poor diploid growth of the triple mutant can be completely overcome by deleting the *RAD51* gene. Importantly, these results implicate Uls1 in the regulation of HR, possibly via the clearance of Rad51 from chromatin (see below). Indeed, we have found that *rad54*Δ *rdh54*Δ *uls1*Δ strains spontaneously accumulate Rad51 foci (7).

To further explore a possible overlap in function between Uls1 and either Rad54 or Rdh54, haploid double mutants *rad54Δ uls1Δ* and *rdh54Δ uls1Δ* were examined for sensitivity to DNA damage. *uls1Δ* did not show a significant increase in DNA damage sensitivity as a single mutant, nor did it enhance the DNA damage sensitivity of a *rdh54Δ* mutant. However, *uls1Δ* did slightly elevate the MMS sensitivity of *rad54Δ* at low MMS doses, providing further support for the idea that Uls1 can partially substitute for Rad54 in DNA damage repair and recombination (Figure 1B).

The above observations are reminiscent of the synthetic lethality that results from combining mutations in genes whose products act to remove Rad51 from DNA

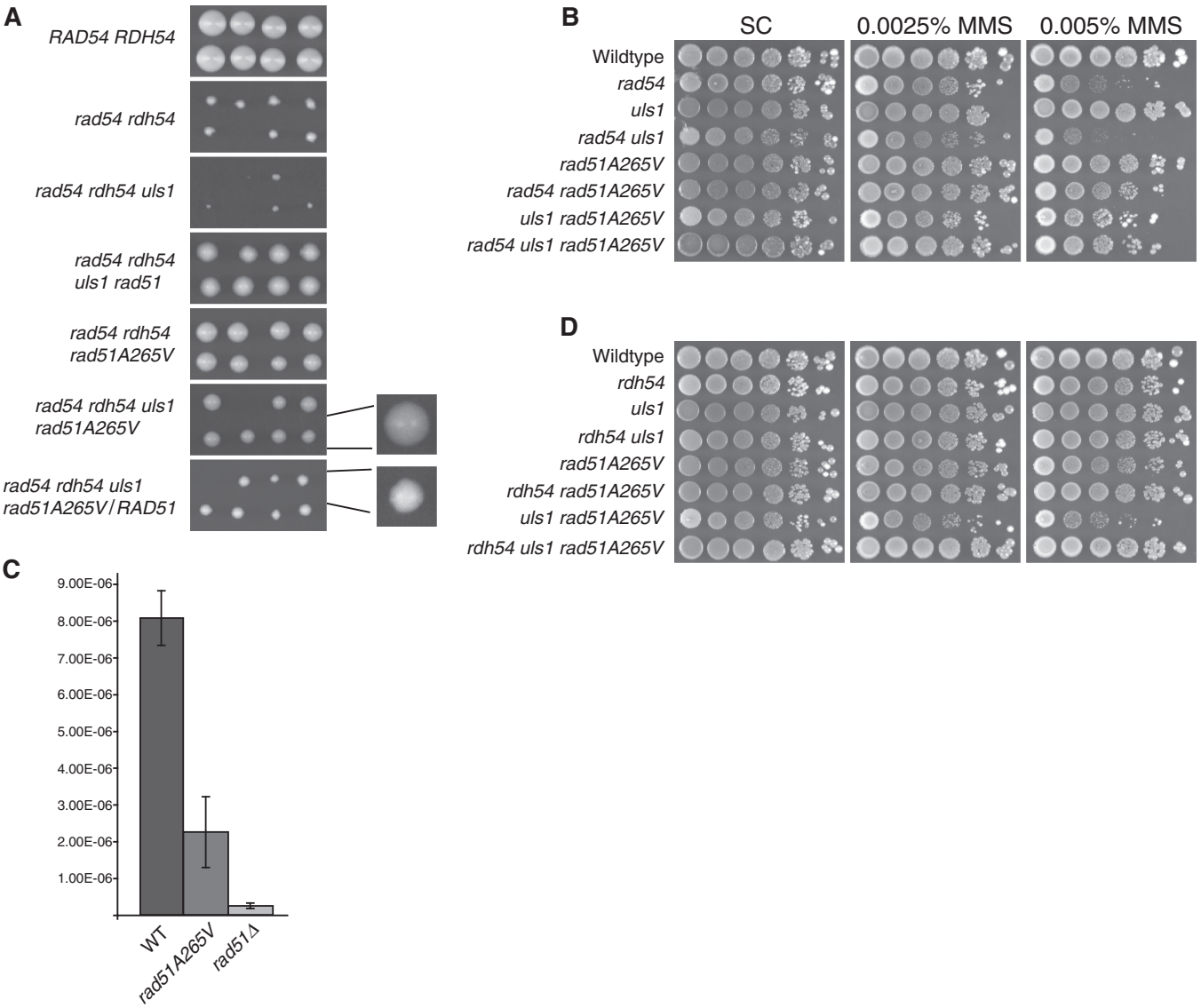

Figure 1. *rad51A265V* suppresses the deleterious effects of multiple Snf/Swi mutants. (**A**) Growth of diploid strains from newly formed zygotes is shown. Pictures were taken after growth on YPD medium at 30°C for 4 days. (**B**) Serial dilution of the indicated haploid strains on SC or SC-containing MMS is shown. Pictures were taken after growth at 30°C for 6 days. (**C**) Gene conversion of an intrachromosomal direct repeat is shown. The recombination system contains *LEU2* heteroalleles separated by the *URA3* marker. Gene conversion events were selected as Leu+ Ura+ segregants. Rates were determined by the median method of the Lea and Coulson fluctuation test. Each test was done of three strains of each genotype. The mean and standard deviation (SD) of these rates are shown. (**D**) Serial dilution of the indicated haploid strains on SC or SC-containing MMS is shown. Pictures were taken after growth at 30°C for 6 days.

combined with other DNA repair factors. The Srs2 DNA helicase can disrupt Rad51 filaments on ssDNA, and mutations in this gene show synthetic lethality with a variety of other mutations, which arise because of the accumulation of toxic recombination intermediates, likely filaments of Rad51 on ssDNA (19). Since Rad54 and Rdh54 remove Rad51 from dsDNA (5,6), we suspected that the poor growth and DNA damage sensitivity of various double and triple mutants, seen in Figure 1, were the result of toxic intermediates generated by persistent association of Rad51 with DNA. We validated this hypothesis via the isolation and characterization of a suppressing mutation in *RAD51*.

Isolation of *rad51A265V* as a suppressor mutation

The enhanced MMS sensitivity of the haploid *rad54Δ uls1Δ* double mutant at low MMS doses provided a means for isolating recessive suppressors, which we reasoned, could be hypomorphic loss-of-function alleles in HR factors. Complete loss-of-function mutations should not rescue the DNA damage sensitivity phenotype, as the HR factors are needed for repairing chromosome damage induced by MMS.

Following EMS mutagenesis of the haploid *rad54Δ uls1Δ* strain, variants of the reduced MMS sensitivity were sought. One such variant displayed enhanced MMS

resistance that was retained in appropriate spore segregants from genetic crosses. Since the suppressor strain had a slight MMS sensitivity in an otherwise wild-type background, we reasoned that it harbors a hypomorphic mutation in a HR gene, possibly *RAD51*. Indeed, sequencing of the chromosomal *RAD51* locus in the suppressor strain revealed the alteration of alanine 265 to valine (change of nucleotide C at position 794 to T). This mutation lies near the subunit interface between adjacent monomers in the Rad51 filament (Figure 2) (20).

To further study the *rad51A265V* mutation, we replaced the wild-type allele with this mutant version in an unmutagenized strain, and used this strain in crosses to generate all of the strain combinations with *rad51A265V* shown in Figure 1A, B and D. Importantly, the *rad51A265V* mutation overcomes the growth deficiency of the *rad54Δ rdh54Δ uls1Δ* diploid (Figure 1A). This suppression is semidominant, as suppression of the growth deficiency of the *rad54Δ rdh54Δ uls1Δ* diploid is seen in *RAD51*/*rad51A265V*, but the suppression is stronger when *rad51A265V* is homozygous. Thus, the *rad51A265V* mutation alleviates the DNA damage sensitivity of the *rad54Δ uls1Δ* double mutant and the growth deficiency of the *rad54Δ rdh54Δ uls1Δ* triple mutant. At low MMS doses, 0.0025 and 0.005%, the *rad51A265V* mutation is epistatic to the *rad54Δ* mutation and suppresses the *rad54Δ* mutation. At higher MMS doses of 0.01 and 0.015%, the *rad51A265V* mutation does not suppress the *rad54Δ* mutation (data not shown).

Genetic assays revealed that the *rad51A265V* strain is reduced in mitotic intrachromosomal gene conversion compared to wild type, although it is still 10-fold higher than the *rad51Δ* rate (Figure 1C). Mitotic interchromosomal gene conversion recombination between homologous chromosomes is not significantly reduced in the *rad51A265V* mutant, whereas it decreases >100-fold in the *rad51Δ* mutant. However, the *rad51A265V* mutation does not suppress the recombination gene conversion defect of *rad54Δ* strains, showing that the *rad51A265V* mutation does not bypass the need for the Rad54 protein in homologous recombination (Supplementary Figure S1).

uls1Δ and *rdh54Δ* show no genetic interaction in a *RAD51* background (Figure 1D). However, the *uls1Δ rad51A265V* double mutant has an enhanced MMS sensitive phenotype. One explanation for this is that Rad54 and Rdh54 compete for the rad51 A265V protein and may prematurely remove the rad51 A265V protein from damage repair sites, thus leading to increased damage sensitivity. To test this, the triple mutant *rdh54Δ uls1Δ rad51 A265V* was examined. Loss of *RDH54* restored MMS resistance to the *uls1Δ rad51A265V* strain. This is consistent with a model in which Rdh54 acts inappropriately on Rad51 dsDNA nucleofilaments to remove Rad51, preventing Rad54 from performing its function in DNA repair. To provide further support for this model, the biochemical properties of the rad51 A265V protein were studied.

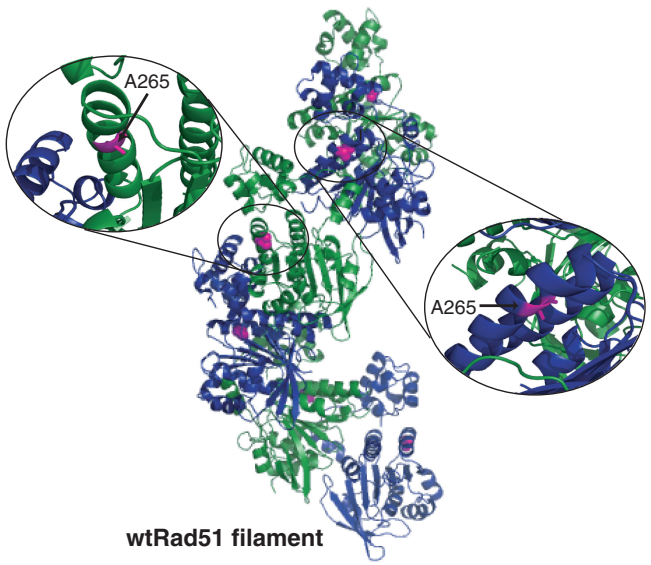

Figure 2. The location of A265V mutation in the Rad51 filament. Rad51 filament structure (20) is represented in blue and green indicating the six monomers that make up a full turn of the filament. Residue A265 is indicated in magenta and the orientation of the residue in the two adjacent monomers is highlighted.

Expression and purification of rad51 A265V mutant protein

To determine if *rad51A265V* encodes a hypomorphic mutant protein that either forms unstable filaments on DNA (hence its suppression of the poor diploid growth of the *rad54Δ rdh54Δ uls1Δ* triple mutant) and/or is more readily removed from dsDNA by Rdh54 (hence its suppression of the DNA damage sensitivity of the *rad54Δ uls1Δ* mutant), we expressed the rad51 A265V mutant protein in yeast cells and purified it (see 'Materials and Methods' section) to near homogeneity (Supplementary Figure S2A) for biochemical characterization (see below). During purification, the rad51 A265V protein exhibited the same chromatographic properties as the wild-type Rad51 protein, and a yield of the mutant protein very similar to that of the wild-type counterpart was obtained.

Characterization of the rad51 A265V mutant protein

Even though the A265V mutation lies near the subunit interface between adjacent monomers in the Rad51 filament (Figure 2), gel filtration analysis showed that the rad51 A265V mutant protein has the same oligomeric structure as wild-type Rad51 in the absence of DNA and ATP (Supplementary Figure S2B). We next tested the purified rad51 A265V mutant alongside wild-type Rad51 for DNA binding, using radiolabeled ssDNA and dsDNA as substrates and mobility shift of these substrates in polyacrylamide gels as assay. Since Rad51 needs ATP to bind DNA, the experiments were conducted in the presence of 2 mM ATP with either 2 or 5 mM $MgCl_2$. As shown in Figure 3A, at 2 mM $MgCl_2$, rad51 A265V is less capable than the wild-type protein in binding ssDNA and dsDNA. This DNA binding deficiency is alleviated to a significant

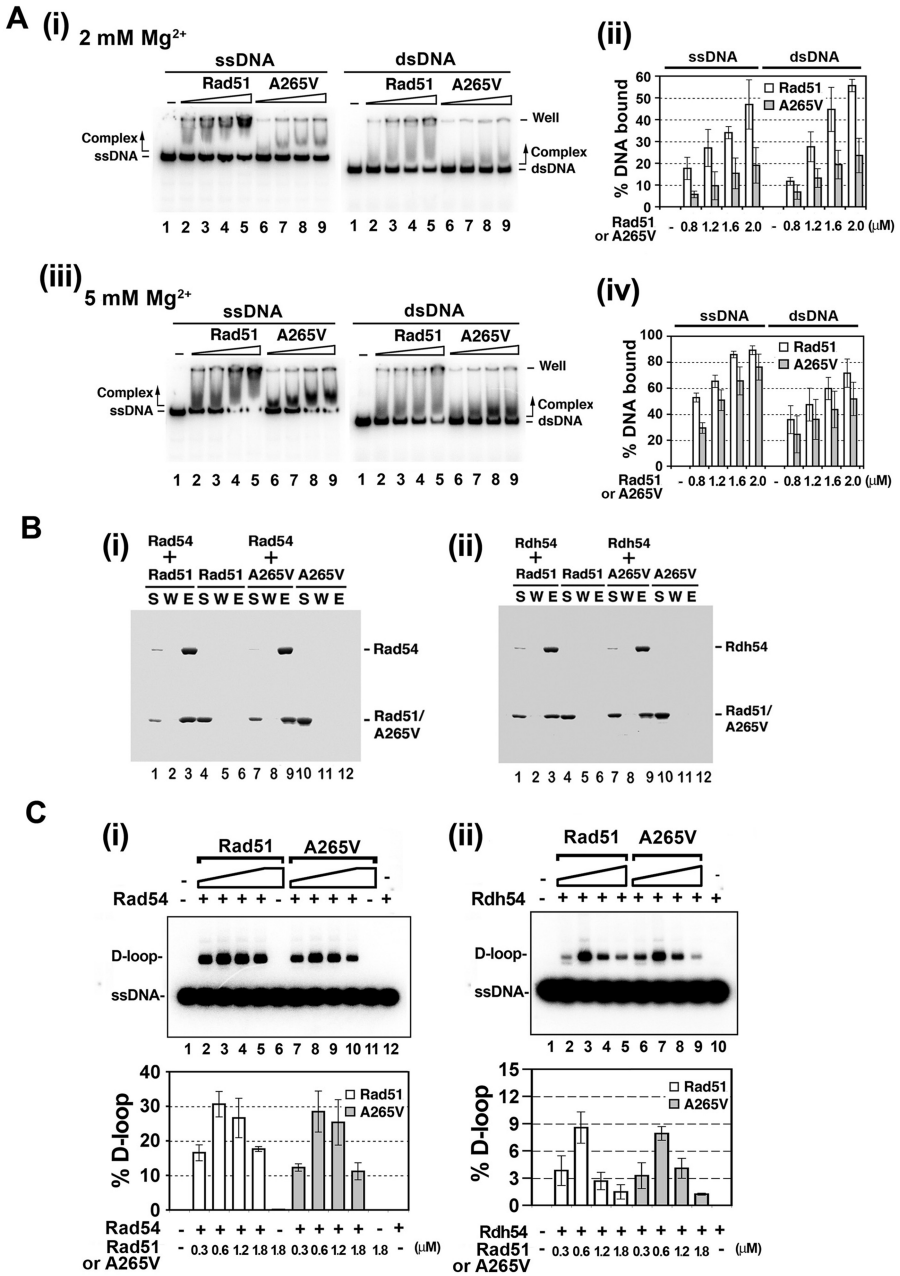

Figure 3. Biochemical attributes of the rad51 A265V mutant protein. (**A**) Rad51 and rad51 A265V proteins (0.8, 1.2, 1.6 and 2.0 μM) were examined for their ability to bind ^{32}P-labeled ssDNA or dsDNA in buffer containing either 2 mM (panel i) or 5 mM (panel iii) $MgCl_2$. The percent DNA bound (complex) was plotted in panel ii (2 mM $MgCl_2$) and panel iv (5 mM $MgCl_2$). Error bars show SD of three experiments. (**B**) Rad51 or rad51 A265V was incubated either alone or with Rad54 (panel i) or Rdh54 (panel ii) and protein complexes were captured on Ni^{2+} NTA-agarose. The beads were washed and then treated with SDS. The supernatant (S), wash (W) and SDS-eluate (E) were analyzed by SDS–PAGE and Coomassie Blue staining. (**C**) Rad51 or rad51 A265V (0.3, 0.6, 1.2 and 1.8 μM) was examined in conjunction with Rad54 (panel i) or Rdh54 (panel ii) for the ability to catalyze the D-loop reaction. Rad51 or rad51 A265V alone (1.8 μM) was also examined (in panel i). The results were plotted. Error bars show SD of three experiments.

degree upon increasing the $MgCl_2$ concentration to 5 mM (Figure 3A).

Duplex DNA becomes extended (by ~50% relative to B form DNA) when bound by Rad51 (1). The use of calf thymus topoisomerase I allows one to register the DNA extension as a topological change; the product of this topoiosmerase-linked reaction is a negatively supercoiled species, called Form UW (Supplementary Figure S3A). In congruence with the results from the DNA mobility shift assay, rad51 A265V was significantly less effective than Rad51 in generating Form UW DNA at 2 mM $MgCl_2$ (Supplementary Figure S3B), whereas a much less pronounced deficit was seen upon increasing the $MgCl_2$ concentration to 5 mM (Supplementary Figure S3C).

Collectively, the results from the DNA mobility shift and topoisomerase-linked assays (Figure 3A and

Supplementary Figure S3), revealed a DNA binding deficiency in rad51 A265V. Additional evidence, presented below, further indicated that rad51 A265V dissociates at a faster rate from dsDNA.

Protein–protein interactions are not affected by the rad51 A265V mutation

In fulfilling its biological role, Rad51 needs to physically and functionally interact with several other factors, including Rad54 and Rdh54. We tested the rad51 A265V mutant for physical interaction with Rad54 and Rdh54 in a pulldown assay that made use of the (His)6 tag on the latter two proteins and nickel NTA agarose beads to capture protein complexes. As shown in Figure 2B, rad51 A265V was just as proficient in interacting with Rad54 or Rdh54 as wild-type Rad51. We further asked whether rad51 A265V retains the ability to functionally synergize with Rad54 or Rdh54 in the D-loop reaction. To do this, a ^{32}P-labeled 90-mer ssDNA was incubated with Rad51 or rad51 A265V before adding Rad54 or Rdh54, followed by the incorporation of the negatively supercoiled homologous duplex target to complete the reaction. Pairing of the ssDNA and homologous duplex yields a ^{32}P-labeled D-loop. Rad54 or Rdh54 greatly enhanced the ability of Rad51 or rad51 A265V to catalyze D-loop formation (Figure 3C).

The above results demonstrated that the A265V mutation has little or no negative impact on Rad51′s interaction with Rad54 or Rdh54 or on its ability to functionally synergize with these Swi2-like factors in catalyzing D-loop formation.

The *rad51A265V* mutation destabilizes the Rad51–dsDNA filament

To ask whether the A265V mutation affects the stability of the Rad51–dsDNA filaments, total internal reflection fluorescence microscopy (TIRFM) was used to monitor the dissociation of the rad51 A265V mutant protein from dsDNA (Figure 4A) (16). To do this, nucleoprotein filaments of either Rad51 or rad51 A265V were assembled on single molecules of dsDNA within the context of a DNA curtain (17). As expected, Rad51 and rad51

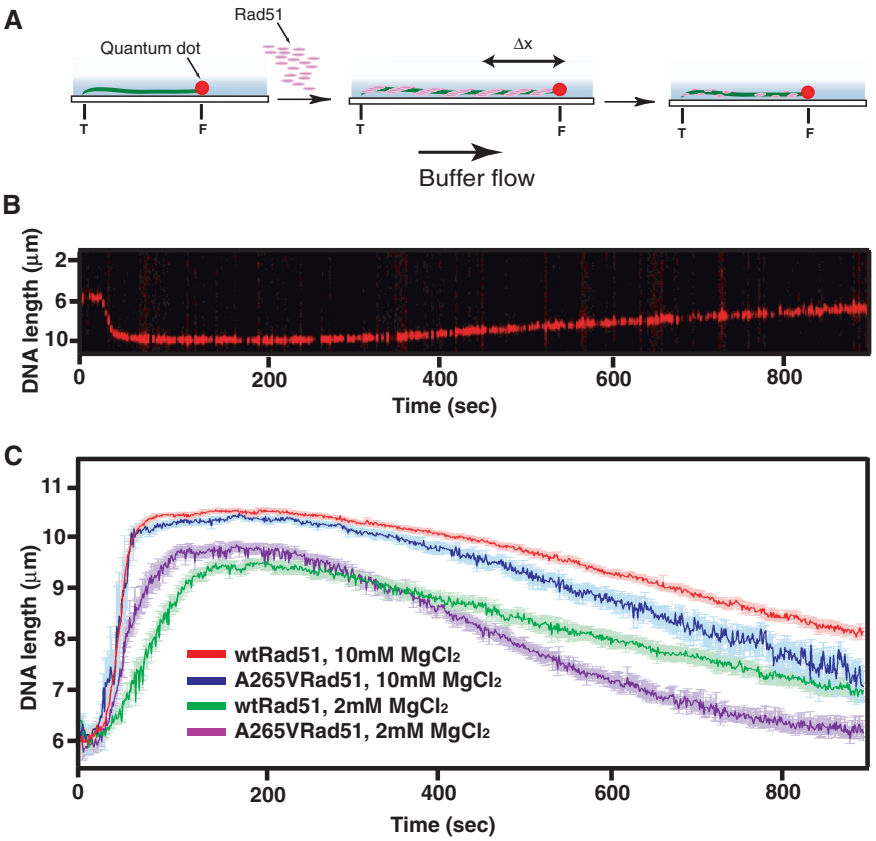

Figure 4. Single-molecule assay of Rad51 and rad51 A265V nucleoprotein filament stability. (**A**) Describes the experimental set-up used to visualize nucleoprotein filament assembly and disassembly. Quantum dot labeled DNA molecules are confined within the evanescent field by application of buffer flow. Rad51 is injected and the quantum dot position is tracked over time. The DNA lengthens (Δx) as Rad51 binds and assembles into a nucleoprotein filament. Disassembly of the filament is then initiated by rinsing with buffer that lacks free Rad51, and contains 2 mM ATP and either 2 or 10 mM $MgCl_2$, as indicated. (**B**) Shows an example of a kymogram with a single DNA molecule as it forms a nucleoprotein filament with rad51 A265V at 10 mM $MgCl_2$. The injection of the protein initiates the rapid lengthening of the DNA. Free protein and ATP are then flushed from the sample chamber at the 200-s mark and the filament begins to disassemble, as indicated by a gradual shortening of the DNA. (**C**) Shows representative tracking data used to quantitate Rad51 filament stability. Each trace represents data obtained from one experiment (~15–20 DNA molecules each), and the disassembly rates reported in the text represent the mean and SD from three independent measurements (~45–60 DNA molecules total). The colors corresponding to different buffer conditions, and either Rad51 or rad51 A265V are indicated.

A265V both extended the length of the DNA by ~68% upon nucleoprotein filament assembly (16,17), and, importantly, rad51 A265V extended the DNA to the same degree as the wild-type protein. This greater than expected increase in the apparent length of the DNA can be attributed to the behavior of the naked DNA versus the nucleoprotein complexes in shear flow; there is an increase in persistence length as Rad51 binds the DNA (21–23), which makes the Rad51-bound DNA easier to stretch at a given flow rate (16,17). These results are in complete agreement with the topological assays presented above (Supplementary Figure S3) confirming that rad51 A265V forms an elongated nucleoprotein filament on dsDNA. The presence of a fluorescent quantum dot at the end of the DNA molecule allowed us to accurately measure the DNA length and quantitate the filament dissociation rate using an automated particle-tracking algorithm, as previously described (24). As shown in Figure 4, the TIRFM analysis provided evidence for a reduced stability of the rad51 A265V nucleoprotein filaments compared to Rad51 filaments. Specifically, at 10 mM $MgCl_2$ wild-type Rad51 filaments disassembled at a rate of 5.6 ± 0.8 nm/s, whereas a more rapid disassembly rate of 7.0 ± 1.1 nm/s was seen for rad51 A265V under the same buffer conditions. At 2 mM $MgCl_2$, the difference in stability was even more pronounced, with an observed value of 5.8 ± 1.1 nm/s for wild type Rad51 compared to 9.9 ± 1.1 nm/s for the mutant protein. These results thus demonstrate that the rad51 A265V mutant is more prone to spontaneously dissociating from dsDNA than wild-type Rad51. Since the turnover of Rad51 from DNA is coupled to ATP hydrolysis, we also tested whether the rad51 A265V mutant has an enhanced ability to hydrolyze ATP. However, results from ATPase assays done in the absence or presence of DNA revealed that the rad51 mutant in fact possesses a slightly attenuated ATPase activity (Supplementary Figure S4).

Accelerated removal of rad51 A265V from dsDNA by Rdh54

The biochemical experiments described earlier (Figure 3) have provided evidence that rad51 A265V has a lower affinity for DNA, which, as indicated from TIRFM experiments, likely stems from a heightened tendency of the mutant protein to dissociate from DNA (Figure 4). Previous studies have found an ability of Rad54 and Rdh54 to remove Rad51 from dsDNA (5,6) and, as noted above, our genetic data have hinted at the possibility that rad51 A265V may be removed from dsDNA at a faster rate by Rdh54. To directly test this premise, we used a biochemical assay, devised previously (5) (Figure 5A), to monitor the dissociation of the Rad51–dsDNA nucleoprotein filament. Briefly, filaments of Rad51 or rad51 A265V were assembled on a biotinylated dsDNA fragment fixed to streptavidin magnetic beads, followed by the addition of Rad54 or Rdh54 together with a non-biotinylated ssDNA molecule to trap the Rad51 molecules that have been dislodged from dsDNA by either of the latter two proteins. As shown before (5,6) and reiterated here, there was a Rad54 or Rdh54 concentration-dependent transfer of Rad51 protein from the magnetic bead-bound DNA to the non-biotinylated ssDNA trap, indicative of dissociation of the Rad51–dsDNA nucleoprotein filament by these Swi2-like factors. Interestingly, while rad51 A265V was removed by Rad54 from the dsDNA at about the same rate as wild-type Rad51 (Figure 5B), a significantly accelerated rate of rad51 A265V dissociation was seen with Rdh54 (Figure 5C). In particular, at the lowest concentration (70 nM) of Rdh54 used, there was a nearly 3-fold difference in susceptibility of the mutant rad51 and wild-type Rad51 filaments to the dissociative action of the former protein (Figure 5C). Taken together, these results suggest that compared to wild-type Rad51 protein, the mutant rad51 A265V protein is more prone to spontaneous dissociation from dsDNA and is also more readily removed from dsDNA by Rdh54.

DISCUSSION

Accumulated Rad51–dsDNA complexes affect cell fitness

With the use of *S. cerevisiae* mutants ablated for the Swi2-related factors Rad54, Rdh54 and Uls1, we have furnished additional evidence that the inability to properly regulate Rad51 nucleoprotein filaments can adversely affect the fitness of mitotic cells. Specifically, haploid and diploid strains deficient in these Swi2-like proteins are sensitive to the DNA damaging agent MMS or are growth impaired, phenotypes that can be overcome via *RAD51* deletion. That the toxicity of Rad51 in the mutant cells stems from gratuitous Rad51–dsDNA complexes is supported by our isolation of the *rad51A265V* suppressor allele and the biochemical demonstration of a reduced stability of the rad51 A265V–dsDNA filament and its enhanced susceptibility to clearance by Rdh54.

Rad51–dsDNA complexes can form either during DSB repair or can arise from nonspecific binding of Rad51 to chromatin. During DSB repair, Rad51–dsDNA complexes are created after DNA strand exchange where the invading single strand coated with Rad51 protein pairs and forms a heteroduplex joint with the homologous duplex partner chromatid. Rad51 removal likely allows DNA polymerases access to the primer terminus for completion of the repair reaction (1,2). Similar to the meiotic recombinase Dmc1, Rad51 accumulates on chromatin and requires translocases to promote its removal from dsDNA, ensuring there is a pool of free protein available when required for DSB repair (7,25). Unlike the bacterial RecA protein, the yeast Rad51 protein displays little binding preference for ssDNA over dsDNA, arguing that recycling mechanisms must come into play if the protein is to be targeted to the correct locations during DSB repair (26–28).

Even though Rad54 and Rdh54 can both remove Rad51 from dsDNA (5,6), unlike Rdh54, Rad54 is no more capable of dissociating rad51 A265V from dsDNA than does wild-type Rad51. Whether this distinction owes to different epitopes on Rad51 being recognized by Rad54 and Rdh54, or to another reason, remains to be delineated, although we suggest that Rad51 bound to

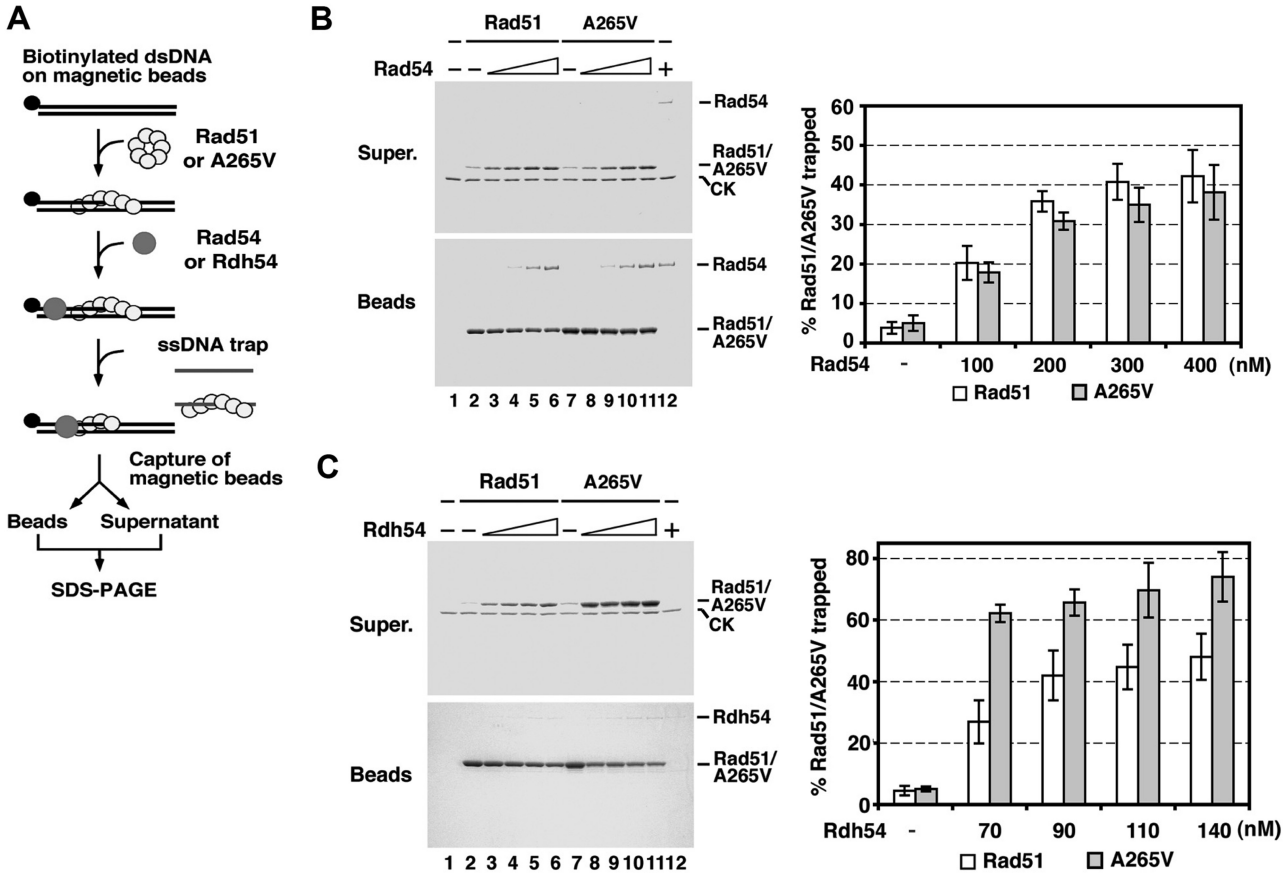

Figure 5. Removal of Rad51 or rad51 A265V from DNA by Rad54 or Rdh54. (**A**) Schematic of the assay. Briefly, filaments of Rad51 or rad51 A265V are assembled on biotinylated dsDNA conjugated to streptavidin magnetic beads. Following an incubation with Rad54 or Rdh54, ssDNA is added to trap Rad51 or rad51 A265V molecules that have been dissociated by Rad54 or Rdh54. The supernatant containing ssDNA and trapped Rad51 or rad51 A265V and the beads containing Rad51 or rad51 A265V that remains on the biotinylated dsDNA are subjected to SDS–PAGE and Coomassie Blue staining. (**B**) and (**C**) Reactions that contained Rad54 (0, 100, 200, 300 and 400 nM in B) or Rdh54 (0, 70, 90, 110 and 140 nM in C) were analyzed and the results were plotted. Error bars show SD of three experiments.

dsDNA at a homologous recombination repair intermediate may differ from Rad51 bound to chromatin (7). Regardless, the differential sensitivities of the rad51 A265V–dsDNA filament to Rad54 and Rdh54 provide evidence for important mechanistic differences in the way these Swi2-like factors act to prevent the non-specific association of Rad51 with bulk chromatin, which is further supported by studies of translocase mutant sensitivity to Rad51 overexpression (7). The damage sensitivity of the *uls1 rad51A265V* mutant may reflect an interference of DNA repair by Rdh54 stemming from the accelerated removal of rad51 A265V mutant protein from a recombination intermediate by this motor protein. An alternative explanation for suppression phenotypes observed in this study may be focused on the action of Rad54 after the formation of a recombination intermediate. Rad54 can promote dissociation of D-loops (29), and this function may be easier to perform with the rad51 A265V protein. In this manner, the *rad51A265V* mutation would prevent the accumulation of recombination intermediates.

We note that genetic studies have revealed other important differences between *RAD54* and *RDH54* as well. Specifically, *RAD54* is more important for DSB repair, DNA extension after strand invasion (30) and haploid recombination than *RDH54,* while *RDH54* makes a more prominent contribution to inter-homologue recombination than to intra-homologue recombination. This suggests that for mitotic DSB repair and recombination, *RAD54* is the frontline translocase that is used in Rad51 removal from dsDNA. The observation that *rad54 rdh54* diploids have a growth defect and are increased in DNA damage sensitivity shows that in diploid mitotic situations, *RDH54* has a role in Rad51 removal, and suggests that it is secondary to *RAD54* for damage repair. In meiosis, *RAD54* and *RDH54* also seem to fulfill distinct roles; Rdh54 interacts with Dmc1 and dissociates Dmc1 from bulk chromatin while Rad54′s action appears to be specific for Rad51 (25,31).

Rad51–ssDNA complexes

In the initial step of the recombination reaction, Rad51 polymerizes onto ssDNA to form the presynaptic filament. Biochemical and genetic studies have provided evidence that the Srs2 helicase regulates recombination outcome and DNA checkpoint signaling by dismantling the Rad51 presynaptic filament (19). Although we believe

that the altered rad51A265V binding to dsDNA is responsible for the suppression phenotypes reported in this article, we found that rad51 A265V also has reduced binding to ssDNA. Consistent with this altered property, we have observed that the synthetic sickness/lethality of *srs2Δ sgs1Δ* (32) and *srs2Δ rad54Δ* (32) haploids is suppressed by the *rad51A265V* mutation (unpublished data). That Rad51 binding to ssDNA may cause some of the *rad54 rdh54 uls1* growth problems remains a possibility, although we note neither Rad54 nor Rdh54 can remove Rad51 from ssDNA. However, it is possible that they might remove Rad51 from secondary structures in ssDNA that resemble dsDNA, and this problem is alleviated by the rad51 A265V mutant.

Uls1 functions in DNA damage repair

That diploid growth becomes severely affected upon introducing the *uls1Δ* deletion into *rad54Δ rdh54Δ* mutant cells suggests that Uls1 protein can function to minimize the toxic accumulation of Rad51 on dsDNA in the absence of Rad54 and Rdh54. Uls1 possesses both Swi2-like DNA translocase motifs and a RING finger domain suggestive of a ubiquitin ligase activity. Whether these activities are germane for Rad51′s removal from dsDNA represent important issues to address in future, although preliminary experiments with the ATPase null show that this mutant version behaves similar to the complete deletion mutant *in vivo*.

Additional *rad51* mutant alleles have been isolated as suppressors of other genetic deficiencies. Some of these *rad51* mutations affect DNA binding or at least lie in regions of Rad51 thought to be involved in DNA binding (33–35). It may be informative to examine these rad51 mutant proteins for their susceptibility to removal from dsDNA by Rad54 and Rdh54. It remains possible that the rad51 mutants that have been recovered from screens for suppressors for DNA damage sensitivity phenotypes and appear to have reduced DNA binding capacity really allow secondary translocases to remove Rad51 protein from DNA and thereby suppress DNA damage sensitivity in the absence of a major factor for DNA damage repair. Such mutant rad51 proteins would be expected to support some degree of DNA repair and recombination, and indeed rad51 A265V fulfills all of these expectations.

Given the high degree of evolutionary conservation of recombination genes (36), our findings could provide the requisite framework for dissecting the role of Rad54 and related proteins, such as Rad54B, in preventing the accumulation of toxic Rad51–dsDNA complexes in human cells. The human *RAD54* gene has been found mutated in tumors (37), and it will be interesting to determine whether any of the tumor-associated hRad54 mutations affect the ability of this protein to remove Rad51 from dsDNA. Additionally, the closest human homolog to the yeast Uls1 protein is SMARCA3/HTLF. Gene silencing of SMARCA3/HTLF has been linked to gastric tumors (38–40), but any connection between hRad54 and SMARCA3/HTLF has not been explored yet. A synergistic enhancement of hRad54 mutations by a SMARCA3/HTLF deletion or knockdown would be indicative of some overlap in function.

SUPPLEMENTARY DATA

Supplementary Data are available at NAR Online.

ACKNOWLEDGEMENTS

The authors thank Lorraine Symington for the gift of plasmids, and the members of the Klein, Sung and Greene laboratories for helpful discussions.

FUNDING

National Institutes of Health (ES007061 to P.S., GM053738 to H.L.K., GM074739 to E.C.G., GM057814 to P.S. and CA146940 to H.L.K, E.C.G. and P.S.). Funding for open access charge: NIH GM053738.

Conflict of interest statement. None declared.

REFERENCES

1. San Filippo,J., Sung,P. and Klein,H. (2008) Mechanism of eukaryotic homologous recombination. *Ann. Rev. Biochem.*, **77**, 229–257.
2. Heyer,W.D., Li,X., Rolfsmeier,M. and Zhang,X.P. (2006) Rad54: the Swiss Army knife of homologous recombination? *Nucleic Acids Res.*, **34**, 4115–4125.
3. Klein,H.L. (1997) RDH54, a RAD54 homologue in *Saccharomyces cerevisiae*, is required for mitotic diploid-specific recombination and repair and for meiosis. *Genetics*, **147**, 1533–1543.
4. Shinohara,A., Gasior,S., Ogawa,T., Kleckner,N. and Bishop,D.K. (1997) *Saccharomyces cerevisiae* recA homologues RAD51 and DMC1 have both distinct and overlapping roles in meiotic recombination. *Genes Cells*, **2**, 615–629.
5. Chi,P., Kwon,Y., Seong,C., Epshtein,A., Lam,I., Sung,P. and Klein,H.L. (2006) Yeast recombination factor Rdh54 functionally interacts with the Rad51 recombinase and catalyzes Rad51 removal from DNA. *J. Biol. Chem.*, **281**, 26268–26279.
6. Solinger,J.A., Kiianitsa,K. and Heyer,W.D. (2002) Rad54, a Swi2/Snf2-like recombinational repair protein, disassembles Rad51:dsDNA filaments. *Mol. Cell*, **10**, 1175–1188.
7. Shah,P.P., Zheng,X., Epshtein,A., Carey,J.N., Bishop,D.K. and Klein,H.L. (2010) Swi2/Snf2-related translocases prevent accumulation of toxic Rad51 complexes during mitotic growth. *Mol. Cell*, **39**, 862–872.
8. Dresser,M.E., Ewing,D.J., Conrad,M.N., Dominguez,A.M., Barstead,R., Jiang,H. and Kodadek,T. (1997) DMC1 functions in a *Saccharomyces cerevisiae* meiotic pathway that is largely independent of the RAD51 pathway. *Genetics*, **147**, 533–544.
9. Lea,D.E. and Coulson,C.A. (1948) The distribution of the numbers of mutants in bacterial populations. *J. Genetics*, **49**, 264–284.
10. Sung,P. and Stratton,S.A. (1996) Yeast Rad51 recombinase mediates polar DNA strand exchange in the absence of ATP hydrolysis. *J. Biol. Chem.*, **271**, 27983–27986.
11. Van Komen,S., Macris,M., Sehorn,M.G. and Sung,P. (2006) Purification and assays of *Saccharomyces cerevisiae* homologous recombination proteins. *Methods Enzymol.*, **408**, 445–463.
12. Raschle,M., Van Komen,S., Chi,P., Ellenberger,T. and Sung,P. (2004) Multiple interactions with the Rad51 recombinase govern the homologous recombination function of Rad54. *J. Biol. Chem.*, **279**, 51973–51980.
13. Petukhova,G., Van Komen,S., Vergano,S., Klein,H. and Sung,P. (1999) Yeast Rad54 promotes Rad51-dependent homologous

DNA pairing via ATP hydrolysis-driven change in DNA double helix conformation. *J. Biol. Chem.*, **274**, 29453–29462.
14. Van Komen,S., Petukhova,G., Sigurdsson,S., Stratton,S. and Sung,P. (2000) Superhelicity-driven homologous DNA pairing by yeast recombination factors Rad51 and Rad54. *Mol. Cell*, **6**, 563–572.
15. Graneli,A., Yeykal,C.C., Prasad,T.K. and Greene,E.C. (2006) Organized arrays of individual DNA molecules tethered to supported lipid bilayers. *Langmuir*, **22**, 292–299.
16. Robertson,R.B., Moses,D.N., Kwon,Y., Chan,P., Chi,P., Klein,H., Sung,P. and Greene,E.C. (2009) Structural transitions within human Rad51 nucleoprotein filaments. *Proc. Natl Acad. Sci. USA*, **106**, 12688–12693.
17. Prasad,T.K., Yeykal,C.C. and Greene,E.C. (2006) Visualizing the assembly of human Rad51 filaments on double-stranded DNA. *J. Mol. Biol.*, **363**, 713–728.
18. Uzunova,K., Gottsche,K., Miteva,M., Weisshaar,S.R., Glanemann,C., Schnellhardt,M., Niessen,M., Scheel,H., Hofmann,K., Johnson,E.S. *et al.* (2007) Ubiquitin-dependent proteolytic control of SUMO conjugates. *J. Biol. Chem.*, **282**, 34167–34175.
19. Sung,P. and Klein,H. (2006) Mechanism of homologous recombination: mediators and helicases take on regulatory functions. *Nat. Rev. Mol. Cell. Biol.*, **7**, 739–750.
20. Conway,A.B., Lynch,T.W., Zhang,Y., Fortin,G.S., Fung,C.W., Symington,L.S. and Rice,P.A. (2004) Crystal structure of a Rad51 filament. *Nat. Struct. Mol. Biol.*, **11**, 791–796.
21. Bennink,M.L., Scharer,O.D., Kanaar,R., Sakata-Sogawa,K., Schins,J.M., Kanger,J.S., de Grooth,B.G. and Greve,J. (1999) Single-molecule manipulation of double-stranded DNA using optical tweezers: interaction studies of DNA with RecA and YOYO-1. *Cytometry*, **36**, 200–208.
22. Egelman,E.H. and Stasiak,A. (1993) Electron microscopy of RecA–DNA complexes: two different states, their functional significance and relation to the solved crystal structure. *Micron*, **24**, 309–324.
23. Hegner,M., Smith,S.B. and Bustamante,C. (1999) Polymerization and mechanical properties of single RecA–DNA filaments. *Proc. Natl Acad. Sci. USA*, **96**, 10109–10114.
24. Prasad,T.K., Robertson,R.B., Visnapuu,M.L., Chi,P., Sung,P. and Greene,E.C. (2007) A DNA-translocating Snf2 molecular motor: Saccharomyces cerevisiae Rdh54 displays processive translocation and extrudes DNA loops. *J. Mol. Biol.*, **369**, 940–953.
25. Holzen,T.M., Shah,P.P., Olivares,H.A. and Bishop,D.K. (2006) Tid1/Rdh54 promotes dissociation of Dmc1 from nonrecombinogenic sites on meiotic chromatin. *Genes Dev.*, **20**, 2593–2604.
26. Ogawa,T., Yu,X., Shinohara,A. and Egelman,E.H. (1993) Similarity of the yeast RAD51 filament to the bacterial RecA filament. *Science*, **259**, 1896–1899.
27. Sung,P. and Robberson,D.L. (1995) DNA strand exchange mediated by a RAD51–ssDNA nucleoprotein filament with polarity opposite to that of RecA. *Cell*, **82**, 453–461.
28. Zaitseva,E.M., Zaitsev,E.N. and Kowalczykowski,S.C. (1999) The DNA binding properties of Saccharomyces cerevisiae Rad51 protein. *J. Biol. Chem.*, **274**, 2907–2915.
29. Bugreev,D.V., Hanaoka,F. and Mazin,A.V. (2007) Rad54 dissociates homologous recombination intermediates by branch migration. *Nat. Struct. Mol. Biol.*, **14**, 746–753.
30. Li,X. and Heyer,W.D. (2009) RAD54 controls access to the invading 3′-OH end after RAD51-mediated DNA strand invasion in homologous recombination in *Saccharomyces cerevisiae*. *Nucleic Acids Res.*, **37**, 638–646.
31. Chi,P., Kwon,Y., Moses,D.N., Seong,C., Sehorn,M.G., Singh,A.K., Tsubouchi,H., Greene,E.C., Klein,H.L. and Sung,P. (2009) Functional interactions of meiotic recombination factors Rdh54 and Dmc1. *DNA Repair*, **8**, 279–284.
32. Klein,H.L. (2001) Mutations in recombinational repair and in checkpoint control genes suppress the lethal combination of srs2Delta with other DNA repair genes in Saccharomyces cerevisiae. *Genetics*, **157**, 557–565.
33. Aboussekhra,A., Chanet,R., Adjiri,A. and Fabre,F. (1992) Semidominant suppressors of Srs2 helicase mutations of *Saccharomyces cerevisiae* map in the RAD51 gene, whose sequence predicts a protein with similarities to procaryotic RecA proteins. *Mol. Cell. Biol.*, **12**, 3224–3234.
34. Chanet,R., Heude,M., Adjiri,A., Maloisel,L. and Fabre,F. (1996) Semidominant mutations in the yeast Rad51 protein and their relationships with the Srs2 helicase. *Mol. Cell. Biol.*, **16**, 4782–4789.
35. Zhang,X.P., Lee,K.I., Solinger,J.A., Kiianitsa,K. and Heyer,W.D. (2005) Gly-103 in the N-terminal domain of *Saccharomyces cerevisiae* Rad51 protein is critical for DNA binding. *J. Biol. Chem.*, **280**, 26303–26311.
36. Krogh,B.O. and Symington,L.S. (2004) Recombination proteins in yeast. *Ann. Rev. Genet.*, **38**, 233–271.
37. Hiramoto,T., Nakanishi,T., Sumiyoshi,T., Fukuda,T., Matsuura,S., Tauchi,H., Komatsu,K., Shibasaki,Y., Inui,H., Watatani,M. *et al.* (1999) Mutations of a novel human RAD54 homologue, RAD54B, in primary cancer. *Oncogene*, **18**, 3422–3426.
38. Hamai,Y., Oue,N., Mitani,Y., Nakayama,H., Ito,R., Matsusaki,K., Yoshida,K., Toge,T. and Yasui,W. (2003) DNA hypermethylation and histone hypoacetylation of the HLTF gene are associated with reduced expression in gastric carcinoma. *Cancer Sci.*, **94**, 692–698.
39. Hibi,K., Nakayama,H., Kanyama,Y., Kodera,Y., Ito,K., Akiyama,S. and Nakao,A. (2003) Methylation pattern of HLTF gene in digestive tract cancers. *Int. J. Cancer*, **104**, 433–436.
40. Moinova,H.R., Chen,W.D., Shen,L., Smiraglia,D., Olechnowicz,J., Ravi,L., Kasturi,L., Myeroff,L., Plass,C., Parsons,R. *et al.* (2002) HLTF gene silencing in human colon cancer. *Proc. Natl Acad. Sci. USA*, **99**, 4562–4567.